



Counter-diffusion biofilms have lower N₂O emissions than co-diffusion biofilms during simultaneous nitrification and denitrification: Insights from depth-profile analysis

Kinh, Co Thi ; Suenaga, Toshikazu ; Hori, Tomoyuki ; Riya, Shohei ; Hosomi, Masaaki ; Smets, Barth F.; Terada, Akihiko

Published in:
Water Research

Link to article, DOI:
[10.1016/j.watres.2017.07.058](https://doi.org/10.1016/j.watres.2017.07.058)

Publication date:
2017

Document Version
Peer reviewed version

[Link back to DTU Orbit](#)

Citation (APA):

Kinh, C. T., Suenaga, T., Hori, T., Riya, S., Hosomi, M., Smets, B. F., & Terada, A. (2017). Counter-diffusion biofilms have lower N₂O emissions than co-diffusion biofilms during simultaneous nitrification and denitrification: Insights from depth-profile analysis. *Water Research*, 124, 363-371. <https://doi.org/10.1016/j.watres.2017.07.058>

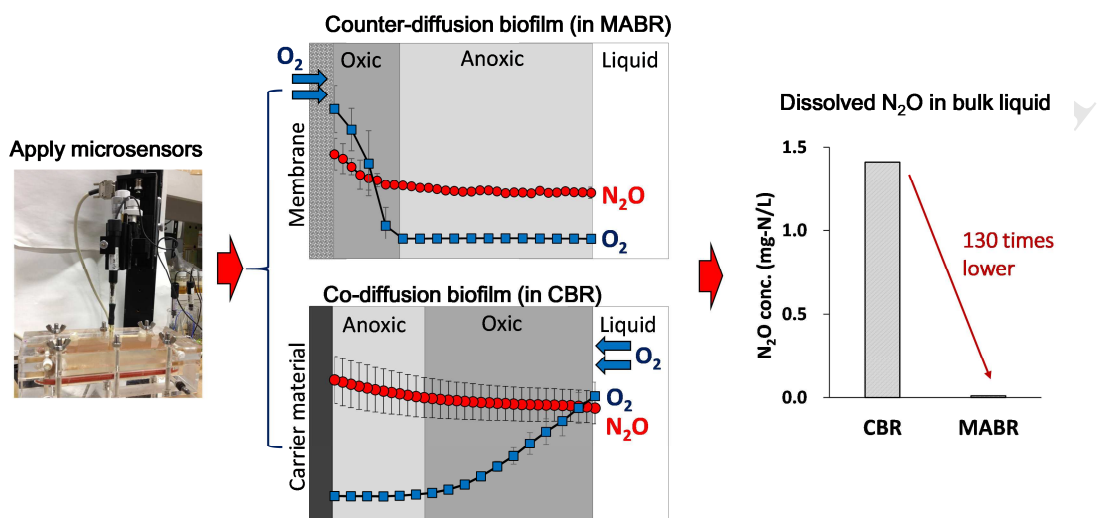
General rights

Copyright and moral rights for the publications made accessible in the public portal are retained by the authors and/or other copyright owners and it is a condition of accessing publications that users recognise and abide by the legal requirements associated with these rights.

- Users may download and print one copy of any publication from the public portal for the purpose of private study or research.
- You may not further distribute the material or use it for any profit-making activity or commercial gain
- You may freely distribute the URL identifying the publication in the public portal

If you believe that this document breaches copyright please contact us providing details, and we will remove access to the work immediately and investigate your claim.

Graphical abstract



Counter-diffusion biofilms have lower N₂O emissions than co-diffusion biofilms during simultaneous nitrification and denitrification: Insights from depth-profile analysis

Co Thi Kinh¹, Toshikazu Suenaga¹, Tomoyuki Hori², Shohei Riya¹, Masaaki Hosomi¹,
Barth F. Smets³, Akihiko Terada*¹

¹Department of Chemical Engineering, Tokyo University of Agriculture and Technology, Naka
2-24-16 Koganei, Tokyo 184-8588, Japan

²Institute for Environmental Management Technology, National Institute of Advanced Industrial
Science and Technology (AIST), Onogawa 16-1, Tsukuba, Ibaraki 305-8569, Japan

³Department of Environmental Engineering, Technical University of Denmark, Miljoevej, 2800
Lyngby, Denmark

Corresponding author: A. Terada (akte@cc.tuat.ac.jp)

Tel/Fax: +81-42-388-7069/+81-42-388-7731

Manuscript submitted to *Water Research*

Keywords: Nitrous oxide, Counter-diffusion biofilm, Microelectrode, Membrane-aerated biofilm reactor, Microbial community

ABSTRACT

1 The goal of this study was to investigate the effectiveness of a membrane-aerated biofilm reactor
2 (MABR), a representative of counter-current substrate diffusion geometry, in mitigating nitrous
3 oxide (N₂O) emission. Two laboratory-scale reactors with the same dimensions but distinct biofilm
4 geometries, *i.e.*, a MABR and a conventional biofilm reactor (CBR) employing co-current substrate
5 diffusion geometry, were operated to determine depth profiles of dissolved oxygen (DO), nitrous
6 oxide (N₂O), functional gene abundance and microbial community structure. Surficial nitrogen
7 removal rate was slightly higher in the MABR (11.0 ± 0.80 g-N/(m²·day) than in the CBR ($9.71 \pm$
8 0.94 g-N/(m²·day), while total organic carbon removal efficiencies were comparable ($96.9 \pm 1.0\%$
9 for MABR and $98.0 \pm 0.8\%$ for CBR). In stark contrast, the dissolved N₂O concentration in the
10 MABR was two orders of magnitude lower (0.011 ± 0.001 mg N₂O-N/L) than that in the CBR (1.38
11 ± 0.25 mg N₂O-N/L), resulting in distinct N₂O emission factors ($0.0058 \pm 0.0005\%$ in the MABR vs.
12 $0.72 \pm 0.13\%$ in the CBR). Analysis on local net N₂O production and consumption rates unveiled
13 that zones for N₂O production and consumption were adjacent in the MABR biofilm. Real-time
14 quantitative PCR indicated higher abundance of denitrifying genes, especially nitrous oxide
15 reductase (*nosZ*) genes, in the MABR versus the CBR. Analyses of the microbial community
16 composition via 16S rRNA gene amplicon sequencing revealed the abundant presence of the genera
17 *Thauera* ($31.2 \pm 11\%$), *Rhizobium* ($10.9 \pm 6.6\%$), *Stenotrophomonas* ($6.8 \pm 2.7\%$), *Sphingobacteria*
18 ($3.2 \pm 1.1\%$) and *Brevundimonas* ($2.5 \pm 1.0\%$) as potential N₂O-reducing bacteria in the MABR.

19 **1. Introduction**

20 Nitrous oxide (N₂O) emission from biological wastewater treatment plants (WWTPs) is of
21 considerable concern because of the extremely high global warming potential and contribution to
22 ozone layer destruction by N₂O (Kampschreur et al. 2009, Law et al. 2012). Implementation of
23 nitrogen-removing technologies, which can attain higher effluent quality and cost effectiveness, is
24 expected to increase the N₂O emitted from biological WWTPs by approximately 13% between
25 2005 and 2020 (IPCC 2007, Itokawa et al. 2001, Okabe et al. 2011). It has been reported that the
26 N₂O impact accounts for up to 78.4% of the total CO₂ footprint in WWTPs (Daelman et al. 2013).
27 Therefore, mitigation of N₂O release from WWTPs is a key challenge.

28 N₂O is produced as a byproduct of nitrification and an intermediate of denitrification.
29 Ammonia-oxidizing bacteria (AOB) or archaea produce N₂O via multiple pathways associated with
30 nitrification and denitrification (Stein and Klotz 2011). Heterotrophic denitrifying bacteria likewise
31 produce N₂O as a result of consecutive enzymatic reactions mediated by nitrate reductase, nitrite
32 reductase and nitric oxide reductase (Morley and Baggs 2010, Philippot 2002, Robertson and
33 Groffman 2015, Schreiber et al. 2012, Wrage et al. 2001, Wunderlin et al. 2012, Zumft 1997). The
34 turnovers of these enzymes are determined by the limited supplies of oxygen for nitrification and of
35 organic carbon for denitrification, affecting the amount of N₂O emission (Kampschreur et al. 2009).
36 Therefore, mitigation strategies to suppress N₂O production have been implemented
37 (Domingo-Félez et al. 2014, Rodriguez-Caballero et al. 2015).

38 Exploiting bacteria possessing nitrous oxide reductase (NosZ), also known as N₂O-reducing
39 bacteria, as a N₂O sink is one mitigation strategy to reduce N₂O emissions from WWTPs
40 (Desloover et al. 2012). The product of NosZ is N₂. Currently, N₂O-reducing bacteria are classified
41 into two clades based on the amino acid sequences of NosZ (Jones et al. 2013, Sanford et al. 2012).
42 Moreover, their physiological traits have been partially determined (Bueno et al. 2015, Desloover et

43 al. 2014, Yoon et al. 2016), extending their potential for application in mitigation of N₂O emissions.
44 Nevertheless, it has been reported that NosZ is the most oxygen-sensitive of denitrifying enzymes
45 (Bonin et al. 1992, Schulthess and Gujer 1996). Thus, provision of anoxic conditions and sufficient
46 amounts of the electron donor and acceptor is of paramount importance in exerting the potential of
47 N₂O-reducing bacteria.

48 Membrane-aerated biofilm reactors (MABR) could be a promising technology capable of
49 enhancing N₂O mitigation. The reactor employs a fixed-film biological treatment technology where
50 a substratum provides oxygen delivery and facilitates biofilm formation (Nerenberg 2016). Oxygen
51 as an electron acceptor is supplied from the biofilm base without bubble formation, whereas
52 electron donors are supplied from the biofilm exterior. Such counter-current substrate diffusion
53 biofilm geometry, in theory, allows two contrasting environments where the electron donor
54 concentration is highest and the oxygen concentration lowest at the biofilm-liquid boundary and
55 *vice versa* at the biofilm-membrane boundary (**Figure S1A**). By utilizing this unique biofilm
56 geometry, a MABR provides a niche in the middle of the biofilm where an electron acceptor
57 co-exists with an electron donor without depletion of either. The niche created in the MABR
58 allowed the occurrence of simultaneous nitrification/denitrification (SND) in a single reactor vessel
59 (Cole et al. 2002, Downing and Nerenberg 2007, 2008b, LaPara et al. 2006, Semmens et al. 2003,
60 Terada et al. 2003). The counter-current substrate diffusion geometry of MABR and its special
61 biofilm niche, in conjunction with bubbleless aeration, could prevent N₂O exhaustion and thus
62 facilitate N₂O mitigation. The mitigation effect has been previously demonstrated in a MABR
63 introducing sequential aeration for partial nitrification (PN)-Anammox (Pellicer-Nacher et al. 2010).
64 Nevertheless, *in situ* evidence of higher N₂O consumption activity has not been obtained in a
65 MABR biofilm.

66 Here, we provide proof of the concept that a MABR for SND can mitigate N₂O emissions. To

67 this end, reactor operation and *in situ* biofilm depth investigation were conducted to reveal: (i)
68 whether a MABR with counter-diffusion biofilm geometry allows the lower amount of N₂O emitted
69 than a conventional biofilm reactor (CBR) with co-diffusion biofilm geometry; (ii) how the spatial
70 distributions of the abundance and activity of N₂O-reducing bacteria vary within the biofilms; and
71 (iii) whether the microbial community structure in the counter-diffusion biofilm is distinct
72 depending on the biofilm depth. To address these research questions, we combined microelectrodes
73 with molecular microbiological methods, *i.e.* quantitative PCR and high-throughput sequencing
74 technology of 16S rRNA gene amplicons, to compare the counter- and co-diffusion biofilms.

75

76 **2. Materials and methods**

77 **2.1. Reactor setup**

78 Two laboratory-scale flow-cell reactors employing counter- and co-diffusion biofilm geometries, a
79 membrane-aerated biofilm reactor (MABR) and a conventional biofilm reactor (CBR) respectively,
80 were operated for 95 days. Each reactor consisted of liquid and gaseous compartments, between
81 which a gas-permeable flat-type silicone membrane (Rubber Co., Tempe, AZ, USA) was inserted.
82 The silicon membrane was 1,000 μm thick and its surface area in each reactor was 41.5 cm^2 . The
83 liquid compartment of each reactor had an effective volume of 0.2 L (specific surface area of the
84 silicone membrane of 20.8 m^2/m^3). The dimensions of both reactors were identical, except that the
85 CBR had a non-permeable plate beneath the silicone membrane (**Figure S2B**). Air was supplied
86 into the two reactors by an air pump (Hiblow, HP100, Saline, MI, USA) with a flow controller. As
87 the entry for oxygen, a bundle of 96 hollow-fibers (MHF3504; Mitsubishi Rayon Co., Ltd., Tokyo,
88 Japan) as a gas permeable membrane was suspended in the liquid phase in the CBR. Whereas the
89 CBR received air via the fiber bundle at an applied pressure of 15 kPa and an air-flow rate of 20

90 mL/min, the MABR received air from the gas compartment (volume 20 mL) via the silicone
91 membrane at 7 kPa and 20 mL/min (**Figure S2A**). Aeration conditions were set based on the
92 preliminary oxygen mass transfer rate estimations (Ahmed et al. 2004). Based on preliminary
93 oxygen transfer tests (data not shown), these conditions provided a comparable oxygen loading rate
94 to the biofilms in the MABR and CBR. The top of both reactors possessed three ports in which
95 microelectrodes were inserted to measure the dissolved N_2O and O_2 concentrations in the biofilms.
96 Synthetic medium, mimicking food-processing wastewater, consisted of CH_3COONa (0.65 g/L),
97 $(NH_4)_2SO_4$ (0.90 g/L) and 100 mL/L of mineral solution comprised of (in mg/L): $MgSO_4 \cdot 7H_2O$
98 (280), KH_2PO_4 (27), $CaCl_2 \cdot 2H_2O$ (120), $NaCl$ (600), $FeSO_4 \cdot 7H_2O$ (3.3), $MnSO_4 \cdot H_2O$ (3.3),
99 $CuCl_2 \cdot 2H_2O$ (0.8), $ZnSO_4 \cdot 7H_2O$ (1.7), and $NiSO_4 \cdot 6H_2O$ (0.3). The medium was sterilized prior to
100 use. The synthetic medium was continuously supplied at 13.8 mL/h by a peristaltic pump
101 (ISMATEC, ISM 930, Wertheim, Germany), ensuring a hydraulic retention time of 14.5 h.
102 Complete mixing was accomplished by a recirculation pump (Masterflex 7553-50, Tokyo, Japan),
103 providing an effective flow rate of 42 mL/s. Effluent samples were collected every few days to
104 evaluate the reactor performances. The fiber bundle in the CBR was cleaned weekly to prevent
105 biofilm growth, so as to maintain constant oxygen supply to the biofilm on the silicone membrane.

106 **2.2. Reactor operation**

107 The two biofilm reactors, *i.e.* the MABR and CBR, were inoculated from a laboratory-scale
108 sequencing batch reactor for partial nitrification (Terada et al. 2013). The inoculum was recirculated
109 in the reactors for 3 days to facilitate bacterial adhesion and biofilm formation. Subsequently, the
110 reactors were fed with synthetic wastewater containing dissolved organic carbon (DOC) and
111 ammonium at concentrations of 190 mg-C/L and 190 mg-N/L, respectively. This condition allowed
112 specific DOC and nitrogen loading rates of 15.1 g-C/(m²·day) and 15.1 g-N/(m²·day), respectively.
113 The temperature was kept at 30°C. pH of the reactors were controlled at 7.0 by addition of $NaHCO_3$.

114 Because denitrification produces alkalinity, which offsets acidity produced via nitrification (Tenno
115 et al. 2016), additional pH control was not necessary. Instead, pH monitoring at every sampling
116 time was carried out in order to verify neutral pH condition in the reactors (7.0 ± 0.2).

117 **2.3. Chemical analysis of influent and effluent wastewater**

118 A sample was filtered through a 0.45- μm pore size membrane (DISMIC-13HP045AN; Advantec,
119 Tokyo, Japan). DOC and total dissolved nitrogen (TDN) concentrations were measured by a TOC
120 analyzer (TOC 5000A, Shimadzu, Kyoto, Japan). Nitrate (NO_3^-), nitrite (NO_2^-) and ammonium
121 (NH_4^+) concentrations were measured using a flow injection analyzer (PE-230, Human Manufacture
122 Engineering, Japan). *t*-test was employed in SPSS 13.0 (IBM Co., New York, USA) to compare
123 DOC and dissolved nitrogen concentrations in the effluents of the two reactors. Dissolved N_2O
124 concentration was measured using a Clark-type microelectrode (Unisense, Aarhus, Denmark). The
125 N_2O emission factor was estimated as the ratio of dissolved N_2O concentration in the bulk liquid to
126 the influent TDN concentration. This factor assumes negligible N_2O exhaustion to the gas phase due
127 to bubbleless aeration, which was confirmed from the gaseous N_2O concentration in the ports for
128 microelectrode insertion, in the gas compartment of the MABR, and in lumens of the hollow-fibers in
129 the CBR.

130 **2.4. Measurement of dissolved O_2 and N_2O concentrations in biofilms**

131 Dissolved N_2O and dissolved oxygen (DO) concentrations throughout the depth of the biofilms
132 were measured using Clark-type microelectrodes (Unisense, Aarhus, Denmark), connected to a
133 picoammeter (MM 3 Microsensor Multimeter, Unisense, Aarhus, Denmark) for data acquisition
134 (Lackner et al. 2010). The diameters of DO and N_2O microelectrodes were 50 μm and 25 μm ,
135 respectively. Calibration of each microelectrode was performed prior to the application to a biofilm
136 according to a previous report (Schreiber et al. 2009). The micromanipulator and microelectrodes

137 were precisely controlled using Sensor Trace Pro software (Unisense, Aarhus, Denmark). Biofilm
138 thicknesses were measured by oxygen concentration profiles. The biofilm depth profiles of N₂O and
139 O₂ concentrations were acquired at 10–15 points from the middle port for microelectrode insertion
140 on days 90 and 95 of reactor operation. The average net volumetric N₂O consumption/production
141 rates by biofilm volume were estimated and averaged from each concentration profile using Fick's
142 second law of diffusion, assuming steady-state conditions (Lorenzen et al. 1999).

143 **2.5. Biomass sectioning**

144 On day 95, each biofilm (approximately 1500 µm thickness) was cut by a scalpel to 0.6 × 0.6 cm
145 and transferred onto a Petri dish with the orientation maintained, as previously described (Terada et
146 al. 2010). Each biofilm was embedded in optimum cutting temperature compound (Tissue-Tek OCT
147 compound, Miles, Elkhart, Ind., IN, USA) overnight to infiltrate the OCT compound into the
148 biofilm, and subsequently frozen at -20°C. The frozen biofilms were horizontally cut into 100
149 µm-thick sections with a cryomicrotome (Cryocut 1800; Leica, Mannheim, Germany) at -20°C and
150 transferred in 1.5-mL microtubes for ensuing DNA extraction.

151 **2.6. DNA extraction, real time PCR, and next generation sequencing by Illumina MiSeq™**

152 DNA extraction was processed using a Fast DNA™ Spin Kit (FastDNA Spin Kit for Soil,
153 MP-Biomedicals, Santa Ana, CA, USA) per the manufacturer's protocol, followed by measurement
154 of DNA concentrations using a spectrophotometer (NanoDrop 2000c, Thermo Scientific,
155 Wilmington, DE, USA). Abundances of functional genes encoding ammonia monooxygenase
156 (bacterial *amoA*), copper and cytochrome *cd*₁-type nitrite reductases (*nirK* and *nirS* respectively),
157 and N₂O reductase (clade I and clade II type *nosZ*) were quantified by real-time quantitative PCR
158 (qPCR) (CFX96 Touch™ Real-Time PCR Detection System, BioRad Laboratories, Hercules, CA,
159 USA). The details of the qPCR procedures are given in Supplementary Information. The PCR

160 conditions were the same as used in previous work (Song et al. 2015).

161 High-throughput sequencing based on 16S rRNA gene amplicons was performed on an
162 Illumina MiSeq platform. The V4 region of 16S rRNA genes was amplified using the primer set
163 515f–806r and the obtained amplicon was subjected to analysis according to the detailed protocol
164 described elsewhere (Aoyagi et al. 2015, Itoh et al. 2014, Schloss et al. 2009) (Supplementary
165 Information). Operational taxonomic units (OTUs) were defined using a threshold of 97% identity.
166 Alpha and beta diversities were calculated by the software QIIME (Caporaso et al. 2010). Principal
167 coordinate analysis was performed based on weighted UniFrac analysis. The sequence data
168 acquired in this study have been deposited in the MG-RAST database
169 (<http://metagenomics.anl.gov/>) named “Counter-diffusion and co-diffusion biofilm for simultaneous
170 nitrification and denitrification reduces N₂O emission” under project ID PSUB006788.

171

172 3. Results

173 3.1. Carbon and nitrogen removal performances of the MABR and CBR

174 Time courses of DOC and nitrogen concentrations are shown in **Figure S3**. According to the trends,
175 the MABR and CBR achieved steady-state performances by day 43 (**Figure S3**). The average
176 effluent concentrations of DOC, TDN, NH₄⁺, NO₂⁻, and NO₃⁻ after day 43 are summarized in
177 **Figure 1**. The average effluent TDN concentration was lower in the MABR (53.7 ± 9.2 mg-N/L)
178 than in the CBR (70.0 ± 10.7 mg-N/L, $p = 5.4 \times 10^{-6}$). Nitrogen removal efficiency was higher in
179 the MABR (72.0 ± 4.8%) than in the CBR (63.5 ± 5.6%, $p = 1.6 \times 10^{-4}$), resulting in specific
180 nitrogen removal rates of 11.0 ± 0.80 and 9.71 ± 0.94 g-N/(m²·day) for the MABR and CBR,
181 respectively. Average effluent DOC concentrations in the two reactors were different, *i.e.*, 5.8 ± 1.8
182 mg/L in the MABR and 3.7 ± 1.5 mg/L in the CBR ($p = 7.0 \times 10^{-3}$). DOC removal performances of

183 the MABR and CBR were both high, at $96.9 \pm 1.0\%$ and $98.0 \pm 0.8\%$, equivalent to specific DOC
184 removal rates of 14.8 ± 0.39 and 15.0 ± 0.38 g-C/(m²-day) for the MABR and the CBR,
185 respectively.

186 *3.2. Depth-profile of DO concentration in biofilms*

187 The depth profiles of DO concentrations in the MABR and CBR on day 95 are shown in **Figures**
188 **2A** and **2B**. On day 95, the TDN concentrations in the MABR and CBR were 39.5 and 72.6
189 mg-N/L, respectively, showing the superior nitrogen removal by the MABR. The biofilm
190 thicknesses were 1400 ± 200 μm in the MABR and 1500 ± 200 μm in the CBR. The DO
191 penetration depth in the MABR (ca. 300 μm) was shallower than that in the CBR (ca. 800 μm),
192 indicating a steep gradient occurred in the MABR biofilm. In the MABR, the DO concentration was
193 highest (2.25 ± 0.5 mg/L) at the biofilm-membrane interface (0 μm) where air was supplied (**Figure**
194 **2A**). In contrast, in the CBR, the DO concentration was higher at the outermost biofilm surface
195 (1.17 ± 0.22 mg/L) and decreased to 0 mg/L at 600 μm from the biofilm-membrane interface
196 (**Figure 2B**).

197 *3.3. Depth-profile of N₂O concentration in biofilms*

198 The gaseous N₂O concentrations in the gas compartment of the MABR and the lumens of the
199 hollow-fiber bundle in the CBR were not distinguishable from the ambient atmospheric N₂O
200 concentrations, indicating negligible levels of N₂O diffusion into the gas compartment (data not
201 shown). N₂O concentration profiles and net volumetric N₂O consumption/production rates in the
202 MABR and CBR are shown in **Figures 2C** and **2D**. The dissolved N₂O concentration at the
203 biofilm-liquid interface in the MABR (0.011 ± 0.001 mg N₂O-N/L) was 130-times lower than that
204 in the CBR (1.38 ± 0.25 mg N₂O-N/L). In the CBR, the highest and lowest N₂O concentrations

205 were respectively detected in the innermost (1.77 ± 0.37 mg N₂O-N/L) and outermost parts ($1.39 \pm$
206 0.25 mg N₂O-N/L) of the biofilm.

207 The depth profile of the net N₂O consumption/production rate in the MABR indicated that N₂O
208 production mainly occurred from 0 to 200 μ m from the biofilm bottom (the biofilm-membrane
209 interface), at rates of 0.0021–0.0043 mg-N/cm³/h varying with biofilm depth. On the contrary, the
210 highest net N₂O consumption rate was observed 250–450 μ m from the biofilm bottom, at a rate of
211 0.0051 mg-N/cm³/h (**Figure 2C**). In the CBR biofilm, the highest N₂O production was observed in
212 the outermost regions (1300–1500 μ m from the biofilm bottom) with the highest rate of 0.034
213 mg-N/cm³/h. In contrast, N₂O consumption was broadly distributed from 0 to 900 μ m, with a rate of
214 0.002–0.02 mg-N/cm³/h. The highest N₂O consumption rate in the CBR was 0.026 mg-N/cm³/h at
215 500 μ m from the biofilm bottom, 5.1 times as high as that in the MABR (0.0051 mg-N/cm³/h). In
216 summary, the MABR biofilm exhibited a lower net N₂O production/consumption rate within a
217 narrower region than the CBR.

218 **3.4. Depth profile of functional gene abundances in biofilms**

219 The depth profiles of the abundances of functional genes for ammonia oxidation (bacterial *amoA*)
220 and denitrification (*nirK*, *nirS*, and clade I/clade II type *nosZ*) in the MABR and CBR are shown in
221 **Figure 3**. The copy numbers of archaeal *amoA* genes were below the detection limit at all locations
222 ($<10^2$ copies/ng-DNA) (data not shown). The abundance of bacterial *amoA* genes in the MABR was
223 generally comparable to that in the CBR: the copy numbers of bacterial *amoA* genes ranged from
224 $2.7\text{--}7.3 \times 10^6$ copies/ng-DNA in the MABR and from $3.2 \times 10^6\text{--}1.1 \times 10^7$ copies/ng-DNA in the CBR.
225 In the MABR, the *amoA* gene abundance was higher in the biofilm interior than in the biofilm
226 exterior by a maximum factor of 2.7 (**Figure 3A**). The opposite trend was obtained in the CBR,
227 where bacterial *amoA* gene abundance was higher in the exterior than in the interior of the biofilm,
228 by a maximum factor of 3.4 (**Figure 3B**).

229 In both the biofilms, *nirK* gene copy numbers were the highest among the examined
230 functional genes, in the order of 10^8 copies/ng-DNA. The *nirK* depth profile in the MABR was
231 irregular, whereas the copy number in the CBR was higher deeper in the biofilm than in the outer
232 (surface) layers (**Figure 3C, D**). The abundance of *nirS* genes was comparable between the MABR
233 and CBR. The trends of *nirS* gene distribution were similar to those of *amoA* genes, *i.e.*, higher *nirS*
234 gene copy numbers were found close to the biofilm bottom in the MABR and at the outermost
235 surface of the biofilm in the CBR (**Figure 3A, B**).

236 The depth profiles of clade I and clade II *nosZ* genes were more pronouncedly stratified in the
237 MABR biofilm than in the CBR biofilm. The abundances of clade I *nosZ* genes at 200–600 μm in
238 the MABR biofilm were higher ($3.3\text{--}4.4 \times 10^6$ copies/ng-DNA) than those in other parts of the
239 biofilm ($1.6\text{--}3.3 \times 10^6$ copies/ng-DNA) (**Figure 3A**). In the CBR, the abundances of clade I *nosZ*
240 genes were relatively constant throughout the biofilm depth, ranging from 1.7×10^6 to 3.1×10^6
241 copies/ng-DNA (**Figure 3B**). The abundances of clade II *nosZ* genes increased by a factor of two
242 from the bottom (0.96×10^5 copies/ng-DNA) to 200 μm (1.9×10^5 copies/ng-DNA) in the MABR
243 biofilm and remained constant with distance above 200 μm (**Figure 3C**). The opposite trend was
244 apparent for clade II *nosZ* gene abundance in the CBR biofilm, *i.e.* decreasing abundance with
245 distance from the biofilm bottom (**Figure 3D**).

246 **3.5. Microbial community structure in the biofilms by Illumina MiSeq sequencing**

247 Alpha-diversities of the MABR and CBR biofilms were comparable and no substantial changes in
248 these diversities were observed within either biofilm (**Table S1, Figures S4 and S5**. For details, see
249 Supplementary Information). **Figure 4** shows the bacterial community composition at the OTU
250 level throughout the biofilm depth. The highly abundant OTUs were identical in the MABR and
251 CBR. However, the relative abundance differed by biofilm depths in the MABR and CBR. The
252 most abundant OTU in both the biofilms was identical to *Thauera mechernichensis* (denovo 33439)

253 of the family Rhodocyclaceae, accounting for $31.2 \pm 11\%$ and $30.3 \pm 4.3\%$ of the total read
254 numbers in the MABR and CBR, respectively. This OTU was especially high in abundance from 0–
255 800 μm in the MABR biofilm, while far less dynamic stratification was observed in the CBR. The
256 second most abundant OTU was *Rhizobium* sp. (denovo 24831) with abundance in the MABR (10.9
257 $\pm 6.6\%$) slightly higher than that in the CBR ($5.2 \pm 1.2\%$). The third to fifth most abundant OTUs
258 were *Stenotrophomonas nitritireducens* (denovo 3270) ($6.8 \pm 2.7\%$ vs. $3.2 \pm 1.5\%$ in the MABR
259 and CBR respectively), *Sphingobacteria* (denovo 25291) ($3.2 \pm 1.1\%$ vs. $2.9 \pm 0.4\%$ in the MABR
260 and CBR respectively), and *Brevundimonas diminuta* (denovo 11916) ($2.5 \pm 1.0\%$ vs. $0.4 \pm 0.5\%$ in
261 the MABR and CBR respectively).

262 A singular AOB, *Nitrosomonas* (denovo 28142), was distributed across the biofilm depth in
263 both systems with relative abundances in the MABR and CBR ranging from 1.5–3.1% and 2.2–
264 5.5%, respectively (**Figure 4**). The abundance of this OTU in both the biofilms decreased after the
265 inoculation; the abundance in the inoculum was 13.7% (**Figure S6**). Far lower abundances of
266 nitrite-oxidizing bacteria (NOB) than AOB were detected in both the MABR and CBR. In addition,
267 no clear spatial distribution of the NOB abundances was observed in either biofilm (**Figure S7**). All
268 the NOB detected were affiliated to *Nitrobacter* spp., and not *Nitrospira* spp.

270 4. Discussion

271 4.1. Far less N_2O emission in the MABR than in the CBR

272 This is the first comprehensive study demonstrating that a MABR emitted far less N_2O than a CBR
273 under operational conditions that give comparative nitrogen removal rates via
274 nitrification/denitrification (**Figures 1** and **2**). After stable operation the reactors since 50 days
275 (**Figure S3**), depth-profiles of O_2 , N_2O and the microbial community structure were determined in
276 both biofilms. The superior TDN removal efficiency obtained in the MABR (**Figure 1** and **S3**)

underscores that a MABR is suitable to achieve SND (Cole et al. 2004, Downing and Nerenberg 2007, LaPara et al. 2006, Nerenberg 2016, Syron and Casey 2008, Terada et al. 2003). The surficial TDN removal rate was 11.0 ± 0.80 g-N/(m²·day) with the removal efficiency of $72.0 \pm 4.8\%$ in the MABR, higher than those of previous reports (1.5 to 9.3 g-N/(m²·day)) with the removal efficiencies of 70-85% (Brindle et al. 1998, Downing and Nerenberg 2008a, Hsieh et al. 2002, Liu et al. 2007, Semmens et al. 2003, Suzuki et al. 2000, Syron et al. 2015, Terada et al. 2003, Walter et al. 2005), likely due to oxygen permeability of the membrane and homogenous biofilm formation onto a planar surface (note that the membrane was a flat-sheet). Here, we show an additional benefit of the MABR, *i.e.*, mitigation of N₂O emission. A N₂O concentration two orders of magnitude lower was observed in the bulk liquid in the MABR compared with the CBR (**Figure 2**). Assuming negligible N₂O exhaustion to the gas phase (note that the aeration mode was bubbleless), N₂O emission factors over the TDN load of the MABR and CBR were $0.0058 \pm 0.0005\%$ and $0.72 \pm 0.13\%$, respectively. While N₂O emission factors have been inconsistently defined, the value in the MABR was much lower than those in previous SND processes, *e.g.*, a hybrid sequencing batch reactor (21% of the nitrogen load) (Lo et al. 2010), a trickling filter system under hypoxia (0.4% of the influent NH₄⁺ load), and stoichiometrically modest methanol-fed conditions (0.2% of the NO₃⁻ load) (Tallec et al. 2006a). The results of our study agree with previous observation of a PN-Anammox MABR, where <0.015% N₂O conversion was noted (Pellicer-Nacher et al. 2010). Nevertheless, we provide the first head-to-head comparison of a CBR with a MABR operated with identical influent loading, with only the biofilm geometry different, which evidences that the MABR is advantageous over the CBR to reduce N₂O emissions.

The far lower N₂O emission from the MABR is likely due to the optimal relative positions of the N₂O production and consumption zones. As **Figure 2C** shows, the hot spots for N₂O production and consumption were at depths of 0–200 and 250–450 μm, respectively. Given that the region for N₂O

301 production roughly coincided with the oxygen penetration depth (**Figure 2A and C**), N₂O was
302 likely produced by AOB, and was immediately reduced to N₂ adjacent to the aerobic zone. N₂O
303 production and consumption rates appeared irregular from 500 to 1400 μm in the MABR, plausibly
304 due to the co-occurrence of N₂O production and consumption mediated by denitrifying bacteria
305 with high turnovers of the consecutive denitrification reactions (note that the values in **Figures 2C**
306 and **2D** are net, rather than absolute). The exterior in a counter-diffusion biofilm for SND confers
307 favorable conditions for denitrification because the DOC is high but oxygen is absent (Matsumoto
308 et al. 2007). This supports our hypothesis on the high denitrification turnover in the biofilm exterior.
309 Taken together, the adjacent positioning of the zones for N₂O production/consumption and the
310 favorable conditions at the biofilm exterior (higher DOC and lower DO concentrations) accelerate
311 N₂O consumption in the MABR biofilm, resulting in the advantage of this reactor in N₂O
312 mitigation.

313 The broader oxygen penetration depth and segregation of the hotspots for N₂O production and
314 consumption may result in higher N₂O production in the CBR (**Figure 2B and D**). Reportedly, a
315 low DO concentration for nitrification and insufficient organic carbon supply for denitrification
316 stimulate N₂O production (Desloover et al. 2012, Kampschreur et al. 2009, Law et al. 2012). Given
317 that DO concentrations were <1 mg/L in a large part of the CBR biofilm (0.01–0.82 mg/L from 0–
318 1400 μm), these hypoxic conditions potentially facilitate N₂O emission from the CBR (Peng et al.
319 2014, Tallec et al. 2006a, Tallec et al. 2006b). In addition to the N₂O production in the broad
320 hypoxic zone, N₂O consumption was observed at 0 to 500 μm (**Figure 2D**). The distance between
321 the hotspots for N₂O production and consumption is disadvantageous because the long distance
322 required for DOC diffusion in the deeper biofilm acts as mass transfer resistance. In co-diffusion
323 biofilms, the highest DOC and oxygen concentrations are found at the uppermost biofilm surface,
324 limiting the DOC available for anoxic respiration including N₂O reduction (Matsumoto et al. 2007).

325 Therefore, the lower DOC concentration in the deeper biofilm of the CBR likely limits N₂O
326 consumption, leading to N₂O accumulation.

327 Another reason for the large difference in the bulk liquid N₂O concentrations could be the
328 difference in DO concentrations at the innermost (2.25 mg/L in **Figure 2C**) and outermost biofilms
329 (1.17 mg/L in **Figure 2D**) in the MABR and CBR. The DO difference was inevitable at the same
330 oxygen loading in both reactors because the CBR forced oxygen to be penetrated through the
331 boundary layer to the biofilm. Ideally, N₂O production in the MABR and CBR should be compared
332 with the same DO concentration at the bottom and top of the respective biofilms. Furthermore, the
333 N₂O production mechanisms and the effects of operational conditions, e.g. pH, temperature,
334 aeration regimes, and DOC/TDN loading rates, on N₂O emission need to be performed in future.

335 **4.2. N₂O reducers in biofilms for SND**

336 Irrespective of the biofilm geometries, *Thauera mechernichensis* was predominant in both the
337 biofilms (**Figure 4**). Despite the lack of genomic information on *T. mechernichensis* so far, it has
338 been reported that *T. mechernichensis* is a canonical denitrifier capable of reducing NO₃⁻ to N₂ via
339 N₂O (Scholten et al. 1999), as demonstrated by other *Thauera* species (Liu et al. 2013), and is
340 present in an nitrogen-removing bioreactor for industrial wastewater treatment (Chang et al. 2011).
341 Given the N₂O consumption potential, *T. mechernichensis* likely reduced N₂O to N₂ at the region
342 from 200 to 300 μm in the MABR biofilm, where N₂O consumption intensively occurred (**Figure**
343 **2C**). Furthermore, this species reportedly reduces NO₃⁻ and NO₂⁻ even at high DO concentrations
344 (Scholten et al. 1999), also confirmed by other species phylogenetically close to *Thauera* species
345 (Liu et al. 2013, Yokoyama et al. 2016). The high abundance of *T. mechernichensis* across a large
346 section of the biofilms, especially from 100–800 μm in the MABR biofilm, suggests its high
347 contribution to denitrification and N₂O consumption. *Rhizobium*, detected in high abundance in the
348 MABR, is also a canonical denitrifier, present in activated sludge, soil, and freshwater environments

349 (Jones et al. 2008, Rochette and Janzen 2005, Wang et al. 2014, Zhao et al. 2013), and most species
350 of the genus *Rhizobium* carry *nosZ* (Rochette and Janzen 2005). Interestingly, the *Rhizobium* OTUs
351 were more abundant in the MABR biofilm exterior than in the interior (**Figure 4A**) and, in contrast,
352 these OTUs were less abundant in the CBR than in the MABR (**Figure 4B**). The physiology of the
353 genus *Rhizobium* remains unclear; however, the higher abundance of this genus in the MABR than
354 in the CBR may be responsible for the greater N₂O consumption of the former, plausibly causing
355 the stark contrast in N₂O emission. Additionally, *Stenotrophomonas nitritireducens* ($6.8 \pm 2.7\%$ on
356 average in samples from the MABR) and *Brevundimonas diminuta* are known N₂O reducers
357 (Finkmann et al. 2000) previously detected in wastewater treatment bioreactors (Chèneby et al.
358 1998, Schweitzer et al. 2001, Srinandan et al. 2011, Yu et al. 2008). Moreover, the *Sphingobacteria*
359 OTU (family Chitinophagaceae) is another denitrifier present in both biofilms (Gabarro et al. 2013,
360 Pan et al. 2013). While more thorough *in situ* analysis on profiles of electron donors and acceptors
361 would be warranted, the better environmental conditions, i.e. the close positions for nitrification and
362 denitrification discussed in 4.1 and the inherent geometry of counter-diffusion biofilm as shown in
363 **Figure S1**, likely facilitated the growth of more abundant potential N₂O-reducing bacteria in the
364 MABR than in the CBR biofilm.

365 **4.3. Implications of functional gene profiles for N₂O reduction**

366 Irrespective of the biofilms in the MABR and CBR, the aerobic regions, as shown in **Figure 2**,
367 showed higher abundances of *amoA* genes than the anoxic zones. The trend was consistent with the
368 depth profiles of *amoA* genes (Cole et al. 2004, LaPara et al. 2006) and the 16S rRNA genes of
369 AOB (Terada et al. 2010) in counter-diffusion biofilms. The relatively higher abundances of clade I
370 and clade II *nosZ* genes in the anoxic regions (300–600 μm and 300–1400 μm , respectively) than in
371 the aerobic part in the MABR biofilm (**Figure 3A** and **C**) indicate that the microaerophilic (0–300
372 μm) and anoxic regions (300 μm -) likely favored the growth of N₂O-reducing bacteria. The absence

373 of DO and corresponding high gene abundances were likewise observed for clade II *nosZ* in the
374 deeper part of the CBR biofilm (**Figure 3D**), but not for clade I *nosZ* (**Figure 3B**). The reason for
375 the incongruence of redox-conditions and gene abundance for clade I *nosZ* could be the limited
376 supply of organic carbon in the influent (C/N ratio = 1) and the inherent geometry of a co-diffusion
377 biofilm, which consumes organic carbon coupled with oxygen respiration. Reportedly, a MABR
378 allows denitrifying bacteria to effectively utilize organic carbon and nitrogen oxides in the middle
379 part of the biofilm (Cole et al. 2004, LaPara et al. 2006). This results in more pronounced gene
380 profiles of clade I *nosZ* genes. Because biokinetic information of N₂O-reducing bacteria is still
381 limited, reasons for selective growth of the N₂O reducers in the anoxic parts of the CBR biofilm
382 entail further investigations.

383 Summarizing these depth profiles of functional genes, redox zonation created in the MABR
384 biofilm permitted more dynamic distribution of AOB and N₂O-reducing bacteria than was found in
385 the CBR biofilm. The closer association of regions for N₂O production and consumption in the
386 MABR biofilm (**Figure 2C**) likely facilitated relay of N₂O plausibly produced by AOB to
387 N₂O-reducing bacteria adjacent to the AOB. This adjacency of these potential N₂O producers and
388 consumers allowed the latter to consume N₂O, resulting in lower N₂O emissions from the MABR.
389 To consolidate this concept, transcription levels of these functional genes, reflecting activities by
390 biofilm depth, and visualization of AOB and N₂O-reducing bacteria in a biofilm, warrant future
391 study.

392

393 5. Conclusions

394 To the best of our knowledge, this is the first report directly comparing a MABR and CBR in terms
395 of overall and spatially resolved N₂O production/reduction and microbial community composition
396 as a function of biofilm depth. The two biofilms, employing counter- and co-current substrate

397 diffusion geometries respectively, were supplied with a high nitrogen-containing wastewater with
398 low DOC/TDN ratio of 1.0 at the same loading rate, and performed simultaneous nitrification and
399 denitrification.

- 400 ● TDN removal efficiency ($72.0 \pm 4.8\%$) was higher in the MABR than in the CBR ($63.5 \pm$
401 5.6%).
- 402 ● Dissolved N_2O concentrations were two orders of magnitude lower in the MABR than in the
403 CBR.
- 404 ● N_2O emission factors of the MABR and CBR, normalized to TDN load, were $0.0058 \pm$
405 0.0005% and $0.72 \pm 0.13\%$, respectively.
- 406 ● The MABR biofilm had narrower regions for N_2O production and consumption than the CBR
407 biofilm.
- 408 ● Higher abundances of denitrifying genes, especially *nosZ*, were observed in the MABR than
409 in the CBR.
- 410 ● Microbial community structure revealed the presence of OTUs affiliated within the genera
411 *Thauera*, *Rhizobium*, *Stenotrophomonas*, *Sphingobacteria* and *Brevundimonas* as potential
412 N_2O -reducing bacteria with higher abundances in the MABR biofilm than in the CBR
413 biofilm.

414 Taking these findings into account, MABRs promise a small-footprint technology achieving both
415 effective simultaneous nitrification/denitrification and mitigation of N_2O emissions.

416

417 ACKNOWLEDGEMENTS

418 We acknowledge Ms. Kanako Mori, Dr. Tomo Aoyagi, Dr. Hirotsugu Fujitan and Prof. Satoshi

419 Tsuneda for technical support in 16S rRNA gene amplicon sequencing and cryosectioning of
420 biofilm samples. This work was supported by a Grant-in-Aid for Scientific Research for Young
421 Scientists (A) (26701009), a Grant-in-Aid for Challenging Exploratory Research (16K12616), a
422 Grand-in-Aid for JSPS Fellows (16J08490) of the Ministry of Education, Culture, Sports, Science
423 and Technology, Japan, the Open Partnership Joint Research Projects (Japan-Denmark) from the
424 Japan Society for the Promotion of Science (JSPS), and the Danish Free Research Council
425 (N2OMAN grant no. DFF-1335-00100).

426

427

428 REFERENCES

429 Ahmed, T., Semmens, M.J. and Voss, M.A. (2004) Oxygen transfer characteristics of hollow-fiber,
430 composite membranes. *Adv Environ Res* 8(3-4), 637-646.

431 Aoyagi, T., Hanada, S., Itoh, H., Sato, Y., Ogata, A., Friedrich, M.W., Kikuchi, Y. and Hori, T.
432 (2015) Ultra-high-sensitivity stable-isotope probing of rRNA by high-throughput sequencing of
433 isopycnic centrifugation gradients. *Environ Microbiol Rep.* 7(2), 282-287.

434 Bonin, P., Gilewicz, M. and Bertrand, J.C. (1992) Effect of oxygen on *Pseudomonas nautica* growth
435 on n-alkane with and without nitrate. *Arch Microbiol* 157, 538-545.

436 Brindle, K., Stephenson, T. and Semmens, M.J. (1998) Nitrification and oxygen utilisation in a
437 membrane aeration bioreactor. *J Membr Sci* 144(1-2), 197-209.

438 Bueno, E., Mania, D., Frostegard, A., Bedmar, E.J., Bakken, L.R. and Delgado, M.J. (2015) Anoxic
439 growth of *Ensifer meliloti* 1021 by N₂O-reduction, a potential mitigation strategy. *Front*
440 *Microbiol* 6, 537.

441 Caporaso, J.G., Kuczynski, J., Stombaugh, J., Bittinger, K., Bushman, F.D., Costello, E.K., Fierer,

- 442 N., Pena, A.G., Goodrich, J.K., Gordon, J.I., Huttley, G.A., Kelley, S.T., Knights, D., Koenig,
443 J.E., Ley, R.E., Lozupone, C.A., McDonald, D., Muegge, B.D., Pirrung, M., Reeder, J.,
444 Sevinsky, J.R., Turnbaugh, P.J., Walters, W.A., Widmann, J., Yatsunenko, T., Zaneveld, J. and
445 Knight, R. (2010) QIIME allows analysis of high-throughput community sequencing data.
446 *Nature Methods* 7(5), 335-336.
- 447 Chang, C.Y., Tanong, K., Xu, J. and Shon, H. (2011) Microbial community analysis of an aerobic
448 nitrifying-denitrifying MBR treating ABS resin wastewater. *Bioresour Technol* 102(9),
449 5337-5344
- 450 Chèneby, D., Hartman, A., Hernault, C., Topp, E. and Germon, J.C. (1998) Diversity of denitrifying
451 microflora and ability to reduce N₂O in two soils. *Biol Fertil Soils* 28, 19-26.
- 452 Cole, A.C., Semmens, M.J. and LaPara, T.M. (2004) Stratification of activity and bacterial
453 community structure in biofilms grown on membranes transferring oxygen. *Appl Environ*
454 *Microbiol* 70(4), 1982-1989.
- 455 Cole, A.C., Shanahan, J.W., Semmens, M. and LaPara, T.M. (2002) Preliminary studies on the
456 microbial community structure of membrane-aerated biofilms treating municipal wastewater.
457 *Desalination* 146, 421-426.
- 458 Daelman, M.R.J., van Voorthuizen, E.M., van Dongen, L.G.J.M., Volcke, E.I.P. and van Loosdrecht,
459 M.C.M. (2013) Methane and nitrous oxide emission from municipal wastewater treatment-
460 results from a long term study. *Water Sci Technol.* 67(10), 2350-2359.
- 461 Desloover, J., Roobroeck, D., Heylen, K., Puig, S., Boeckx, P., Verstraete, W. and Boon, N. (2014)
462 Pathway of nitrous oxide consumption in isolated *Pseudomonas stutzeri* strains under anoxic
463 and oxic conditions. *Environ Microbiol* 16(10), 3143-3152.
- 464 Desloover, J., Vlaeminck, S.E., Clauwaert, P., Verstraete, W. and Boon, N. (2012) Strategies to
465 mitigate N₂O emissions from biological nitrogen removal systems. *Curr Opin Biotechnol* 23(3),

- 466 474-482.
- 467 Domingo-Félez, C., Mutlu, A.G., Jensen, M.M. and Smets, B.F. (2014) Aeration strategies to
468 mitigate nitrous oxide emissions from single-stage nitrification/anammox reactors. *Environ Sci*
469 *Technol* 48(15), 8679-8687.
- 470 Downing, L.S. and Nerenberg, R. (2007) Performance and microbial ecology of the hybrid
471 membrane biofilm process for concurrent nitrification and denitrification of wastewater. *Water*
472 *Sci Technol* 55(8-9), 355.
- 473 Downing, L.S. and Nerenberg, R. (2008a) Effect of bulk liquid BOD concentration on activity and
474 microbial community structure of a nitrifying, membrane-aerated biofilm. *Appl Microbiol*
475 *Biotechnol* 81(1), 153-162.
- 476 Downing, L.S. and Nerenberg, R. (2008b) Total nitrogen removal in a hybrid, membrane-aerated
477 activated sludge process. *Water Res* 42(14), 3697-3708.
- 478 Etchebehere, C. and Tiedje, J. (2005) Presence of two different active nirS nitrite reductase genes in
479 a denitrifying *Thauera* sp. from a high-nitrate-removal-rate reactor. *Appl Environ Microbiol*
480 71(9), 5642-5645.
- 481 Finkmann, W., Altendorf, K., Stackebrandt, E. and Lipski, A. (2000) Characterization of
482 N₂O-producing Xanthomonas-like isolates from biofilters as *Stenotrophomonas nitritireducens*
483 *sp. nov.*, *Luteimonas mephitis gen. nov., sp. nov.* and *Pseudoxanthomonas broegbernensis gen.*
484 *nov., sp. nov.* *Int J Syst Evol Microbiol* 50, 273-282.
- 485 Gabarro, J., Hernandez-Del Amo, E., Gich, F., Rusalleda, M., Balaguer, M.D. and Colprim, J.
486 (2013) Nitrous oxide reduction genetic potential from the microbial community of an
487 intermittently aerated partial nitrification SBR treating mature landfill leachate. *Water Res*
488 47(19), 7066-7077.
- 489 Hsieh, Y. L., Tseng, S.K. and Chang, Y. J. (2002) Nitrification using polyvinyl alcohol-immobilized

- 490 nitrifying biofilm on an O₂-enriching membrane. *Biotechnol Lett* 24, 315–319.
- 491 IPCC (2007) Summary for Policy-makers, *Climate Change 2007: Mitigation. Contribution of*
492 *Working Group III to the Fourth Assessment Report of the IPCC.* In B. Metz, O.R. Davidson,
493 P.R. Bosch, R. dave, L.A. Meyer eds. . Cambridge University Press, Cambridge, United
494 Kingdom and New York, NY, USA.
- 495 Itoh, H., Navarro, R., Takeshita, K., Tago, K., Hayatsu, M., Hori, T. and Kikuchi, Y. (2014)
496 Bacterial population succession and adaptation affected by insecticide application and soil
497 spraying history. *Front Microbiol* 5(457), 1-12.
- 498 Itokawa, H., Hanaki, K. and Matsuo, T. (2001) Nitrous oxide production in high-loading biological
499 nitrogen removal process under low COD/N ratio condition. *Water Res* 35(3), 657-664.
- 500 Jones, C.M., Graf, D.R., Bru, D., Philippot, L. and Hallin, S. (2013) The unaccounted yet abundant
501 nitrous oxide-reducing microbial community: a potential nitrous oxide sink. *ISME J* 7(2),
502 417-426.
- 503 Jones, C.M., Stres, B., Rosenquist, M. and Hallin, S. (2008) Phylogenetic analysis of nitrite, nitric
504 oxide, and nitrous oxide respiratory enzymes reveal a complex evolutionary history for
505 denitrification. *Mol Biol Evol* 25(9), 1955-1966.
- 506 Kampschreur, M.J., Temmink, H., Kleerebezem, R., Jetten, M.S. and van Loosdrecht, M.C. (2009)
507 Nitrous oxide emission during wastewater treatment. *Water Res* 43(17), 4093-4103.
- 508 LaPara, T.M., Cole, A.C., Shanahan, J.W. and Semmens, M.J. (2006) The effects of organic carbon,
509 ammoniacal-nitrogen, and oxygen partial pressure on the stratification of membrane-aerated
510 biofilms. *J Ind Microbiol Biotechnol* 33(4), 315-323.
- 511 Law, Y., Ye, L., Pan, Y. and Yuan, Z. (2012) Nitrous oxide emissions from wastewater treatment
512 processes. *Philos Trans R Soc Lond B* (367), 1265-1277.
- 513 Liu, B., Mao, Y., Bergaust, L., Bakken, L.R. and Frostegard, A. (2013) Strains in the genus *Thauera*

- 514 exhibit remarkably different denitrification regulatory phenotypes. *Environ Microbiol* 15(10),
515 2816-2828.
- 516 Liu, H., Yang, F., Wang, T., Liu, Q. and Hu, S. (2007) Carbon membrane-aerated biofilm reactor for
517 synthetic wastewater treatment. *Bioprocess Biosyst Eng* 30(4), 217-224.
- 518 Lorenzen, J., Larsen, L.H., Kjaer, T. and Revsbech, N. (1999) Biosensor determination of the
519 microscale distribution of nitrate, nitrate assimilation, nitrification, and denitrification in a
520 diatom-inhabited freshwater sediment. *Appl Environ Microbiol* 64(9), 3264-3269.
- 521 Matsumoto, S., Terada, A. and Tsuneda, S. (2007) Modeling of membrane-aerated biofilm: Effects
522 of C/N ratio, biofilm thickness and surface loading of oxygen on feasibility of simultaneous
523 nitrification and denitrification. *Biochem Eng J* 37(1), 98-107.
- 524 Morley, N. and Baggs, E.M. (2010) Carbon and oxygen controls on N₂O and N₂ production during
525 nitrate reduction. *Soil Biol Biochem* 42(10), 1864-1871.
- 526 Nerenberg, R. (2016) The membrane-biofilm reactor (MBfR) as a counter-diffusional biofilm
527 process. *Curr Opin Biotechnol* 38, 131-136.
- 528 Okabe, S., Oshiki, M., Takahashi, Y. and Satoh, H. (2011) N₂O emission from a partial
529 nitrification-anammox process and identification of a key biological process of N₂O emission
530 from anammox granules. *Water Res* 45(19), 6461-6470.
- 531 Pan, Y., Ni, B.J., Bond, P.L., Ye, L. and Yuan, Z. (2013) Electron competition among nitrogen
532 oxides reduction during methanol-utilizing denitrification in wastewater treatment. *Water Res*
533 47(10), 3273-3281.
- 534 Pellicer-Nacher, C., Sun, S., Lackner, S., Terada A., Schreiber, F. and Smets, B. (2010) Sequential
535 aeration of membrane-aerated biofilm reactors for high-rate autotrophic nitrogen removal:
536 experimental demonstration. *Environ. Sci. Technol.* 44, 7628-7634.
- 537 Peng, L., Ni, B.J., Erler, D., Ye, L. and Yuan, Z. (2014) The effect of dissolved oxygen on N₂O

- 538 production by ammonia-oxidizing bacteria in an enriched nitrifying sludge. *Water Res* 66,
539 12-21.
- 540 Philippot, L. (2002) Denitrifying genes in bacterial and Archaeal genomes. *Biochimica et*
541 *Biophysica Acta* 1577, 355-376.
- 542 Robertson, G.P. and Groffman, P.M. (2015) Nitrogen transformations. In B. Metz, O.R. Davidson,
543 P.R. Bosch, R. Dave, L.A. Meyer eds. Cambridge E. A. Paul, editor. *Soil microbiology, ecology*
544 *and biochemistry*. 4th edition. Academic Press, 421-446.
- 545 Rochette, P. and Janzen, H.H. (2005) Towards a revised coefficient for estimating N₂O emissions
546 from legumes. *Nutr Cycl Agroecosys* 73(2-3), 171-179.
- 547 Rodriguez-Caballero, A., Aymerich, I., Marques, R., Poch, M. and Pijuan, M. (2015) Minimizing
548 N₂O emissions and carbon footprint on a full-scale activated sludge sequencing batch reactor.
549 *Water Res* 71, 1-10.
- 550 Sanford, R.A., Wagner, D.D., Wu, Q., Chee-Sanford, J.C., Thomas, S.H., Cruz-Garcia, C.,
551 Rodriguez, G., Massol-Deya, A., Krishnani, K.K., Ritalahti, K.M., Nissen, S., Konstantinidis,
552 K.T. and Löffler, F.E. (2012) Unexpected nondenitrifier nitrous oxide reductase gene diversity
553 and abundance in soils. *Proc Natl Acad Sci USA* 109(48), 19709-19714.
- 554 Schloss, P.D., Westcott, S.L., Ryabin, T., Hall, J.R., Hartmann, M., Hollister, E.B., Lesniewski,
555 R.A., Oakley, B.B., Parks, D.H., Robinson, C.J., Sahl, J.W., Stres, B., Thallinger, G.G., Van
556 Horn, D.J. and Weber, C.F. (2009) Introducing mothur: open-source, platform-independent,
557 community-supported software for describing and comparing microbial communities. *Appl*
558 *Environ Microbiol* 75(23), 7537-7541.
- 559 Scholten, T., Lukow, T., Auling, G., Kroppenstedt, M., Rainey, F.A. and Deikmann, H. (1999)
560 *Thauera mechernichensis* sp. nov., an aerobic denitrifier from a leachate treatment plant. *Int J*
561 *Syst Bacteriol* 49, 1045–1051.

- 562 Schreiber, F., Loeffler, B., Polerecky, L., Kuypers, M.M. and de Beer, D. (2009) Mechanisms of
563 transient nitric oxide and nitrous oxide production in a complex biofilm. *ISME J* 3(11),
564 1301-1313.
- 565 Schreiber, F., Wunderlin, P., Udert, K.M. and Wells, G.F. (2012) Nitric oxide and nitrous oxide
566 turnover in natural and engineered microbial communities: biological pathways, chemical
567 reactions, and novel technologies. *Front Microbiol* 3, 372.
- 568 Schulthess, R.V. and Gujer, W. (1996) Release of nitrous oxide (N₂O) from denitrifying activated
569 sludge: verification and application of a mathematical model. *Water Res* 30(3), 521-530.
- 570 Schweitzer, B., Huber, I., Amann, R., Ludwig, W. and Simon, M. (2001) Alpha- and
571 beta-Proteobacteria control the consumption and release of amino acids on lake snow
572 aggregates. *Appl Environ Microbiol* 67(2), 632-645.
- 573 Semmens, M.J., Dahm, K., Shanahan, J. and Christianson, A. (2003) COD and nitrogen removal by
574 biofilms growing on gas permeable membranes. *Water Res* 37(18), 4343-4350.
- 575 Song, K., Suenaga, T., Harper, W.F., Jr., Hori, T., Riya, S., Hosomi, M. and Terada, A. (2015)
576 Effects of aeration and internal recycle flow on nitrous oxide emissions from a modified
577 Ludzak-Ettinger process fed with glycerol. *Environ Sci Pollut Res* 22(24), 19562-19570.
- 578 Srinandan, C.S., Shah, M., Patel, B. and Nerurkar, A.S. (2011) Assessment of denitrifying bacterial
579 composition in activated sludge. *Bioresour Technol* 102(20), 9481-9489.
- 580 Stein, L.Y. and Klotz, M.G. (2011) Nitrifying and denitrifying pathways of methanotrophic bacteria.
581 *Biochem Soc Trans* 39(6), 1826-1831.
- 582 Suzuki, Y., Hatano, N., Ito, S. and Ikeda, H. (2000) Performance of nitrogen removal and biofilm
583 structure of porous gas permeable membrane reactor. *Water Sci Technol* 41(4-5), 211-217.
- 584 Syron, E. and Casey, E. (2008) Membrane-aerated biofilms for high rate biotreatment: performance
585 appraisal, engineering principles, scale-up, and development requirements. *Environ Sci Technol*

- 586 42(6), 1833-1844.
- 587 Syron, E., Semmens, M.J. and Casey, E. (2015) Performance analysis of a pilot-scale membrane
588 aerated biofilm reactor for the treatment of landfill leachate. *Chem Eng J* 273, 120-129.
- 589 Tallec, G., Garnier, J., Billen, G. and Gousailles, M. (2006a) Nitrous oxide emissions from
590 secondary activated sludge in nitrifying conditions of urban wastewater treatment plants: effect
591 of oxygenation level. *Water Res* 40(15), 2972-2980.
- 592 Tallec, G., Garnier, J. and Gousailles, M. (2006b) Nitrogen removal in a wastewater treatment plant
593 through biofilters: nitrous oxide emissions during nitrification and denitrification. *Bioprocess*
594 *Biosyst Eng* 29(5-6), 323-333.
- 595 Tenno, T., Zekker, I., Rikmann, E., Tenno, T., Daija, L. and Mashirin, A. (2016) Modelling
596 equilibrium distribution of carbonaceous ions and molecules in a heterogeneous system of
597 CaCO_3 -water-gas. *P Est Acad Sci* 65(1), 68.
- 598 Terada, A., Hibiya, K., Nagai, J., Tsuneda, S. and Hirata, A. (2003) Nitrogen removal characteristics
599 and biofilm analysis of a membrane-aerated biofilm reactor applicable to high-strength
600 nitrogenous wastewater treatment. *J Biosci Bioeng* 95(2), 170-178.
- 601 Terada, A., Sugawara, S., Yamamoto, T., Zhou, S., Koba, K. and Hosomi, M. (2013) Physiological
602 characteristics of predominant ammonia-oxidizing bacteria enriched from bioreactors with
603 different influent supply regimes. *Biochem Eng J* 79, 153-161.
- 604 Terada, A., Lackner, S., Kristensen, K. and Smets, B.F. (2010) Inoculum effects on community
605 composition and nitrification performance of autotrophic nitrifying biofilm reactors with
606 counter-diffusion geometry. *Environ Microbiol* 12(10), 2858-2872.
- 607 Walter, B., Haase, C. and Rabiger, N. (2005) Combined nitrification/denitrification in a membrane
608 reactor. *Water Res* 39(13), 2781-2788.
- 609 Wang, Z., Zhang, X., Lu, X., Liu, B., Li, Y., Long, C. and Li, A. (2014) Abundance and diversity of

- 610 bacterial nitrifiers and denitrifiers and their functional genes in tannery wastewater treatment
611 plants revealed by high-throughput sequencing. *PLoS One* 9(11), 1-19.
- 612 Wrage, N., Velthol, G.L., Beusichem, M.L. and Oenema, O. (2001) Role of nitrifier denitrification
613 in the production of nitrous oxide. *Soil Biol Biochem* 33, 1723-1732.
- 614 Wunderlin, P., Mohn, J., Joss, A., Emmenegger, L. and Siegrist, H. (2012) Mechanisms of N₂O
615 production in biological wastewater treatment under nitrifying and denitrifying conditions.
616 *Water Res* 46(4), 1027-1037.
- 617 Yokoyama K, Yumura M, Honda T, Ajitomi E (2016) Characterization of denitrification and net
618 N₂O-reduction properties of novel aerobically N₂O-reducing bacteria. *Soil Sci Plant Nutr* 62,
619 230-239.
- 620 Yoon, S., Nissen, S., Park, D., Sanford, R.A. and Löffler, F.E. (2016) Nitrous oxide reduction
621 kinetics distinguish bacteria harboring clade I versus clade II NosZ. *Appl Environ Microbiol*
622 82(13), 3793-3800.
- 623 Yu, I.S., Yeom, S.J., Kim, H.J., Lee, J.K., Kim, Y.H. and Oh, D.K. (2008) Substrate specificity of
624 *Stenotrophomonas nitritireducens* in the hydroxylation of unsaturated fatty acid. *Appl*
625 *Microbiol Biotechnol* 78(1), 157-163.
- 626 Zhao, Y., Huang, J., Zhao, H. and Yang, H. (2013) Microbial community and N removal of aerobic
627 granular sludge at high COD and N loading rates. *Bioresour Technol* 143, 439-446.
- 628 Zumft, W. (1997) Cell biology and molecular basis of denitrification. *Microbiol Mol Biol Rev*
629 61(4), 533-616.

630

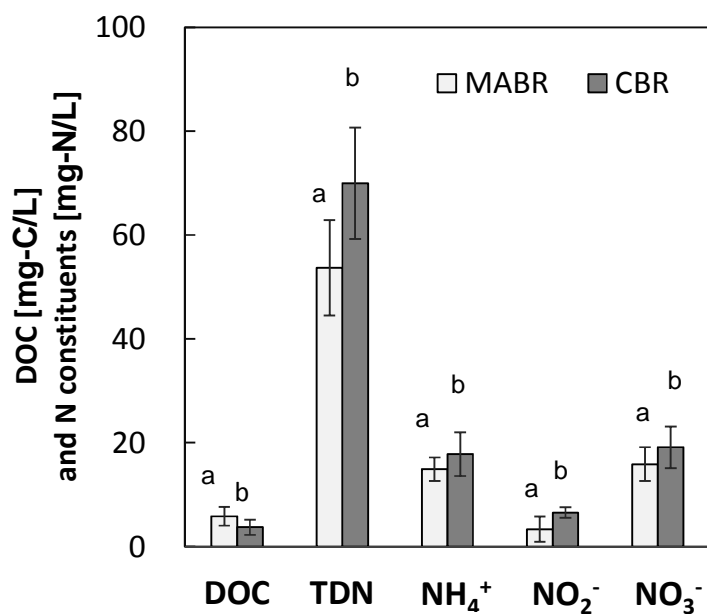


Figure 1. Average concentrations in effluent of dissolved organic carbon (DOC), total dissolved nitrogen (TDN), ammonium (NH₄⁺), nitrite (NO₂⁻), and nitrate (NO₃⁻) in the steady state (day 43–95) in the MABR and CBR. Different letters for each constituent indicate a significant difference ($p < 0.05$) between the MABR and CBR.

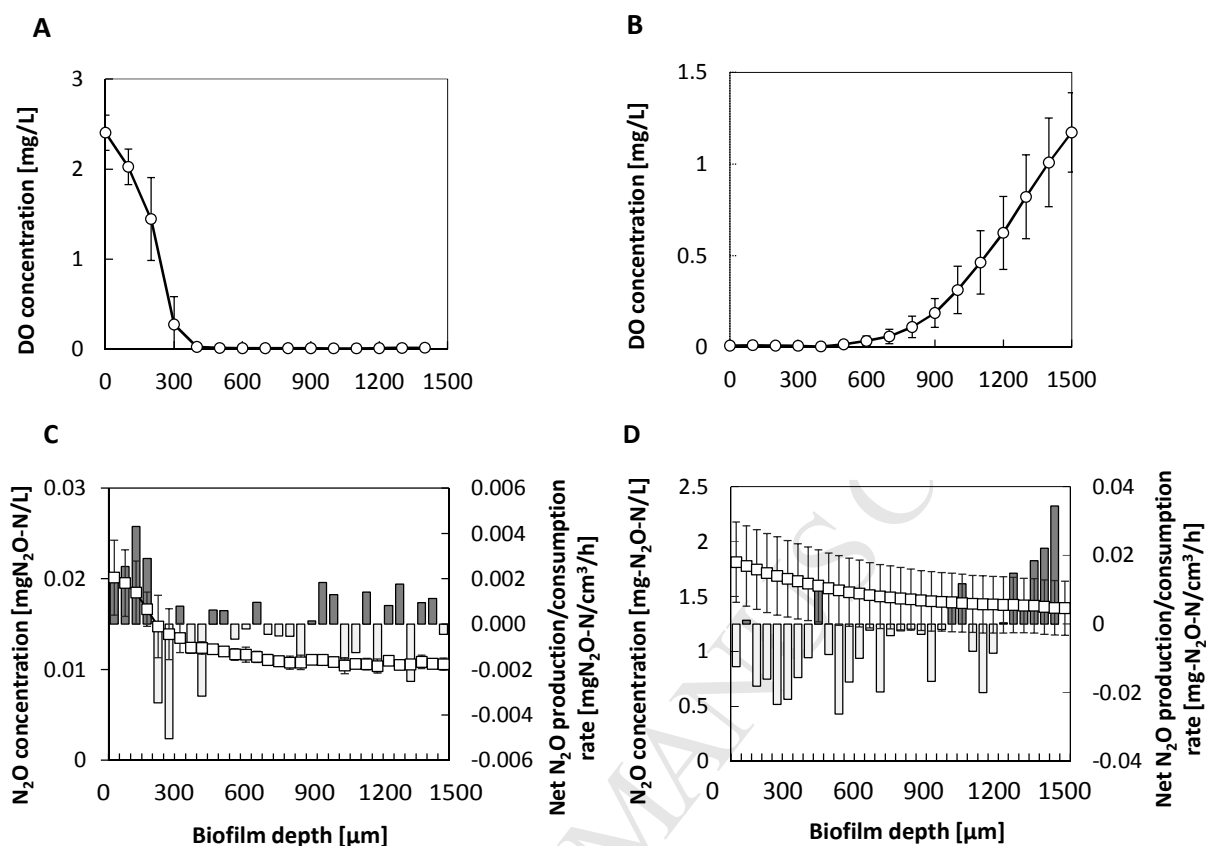


Figure 2. Depth profiles of O₂ and N₂O concentrations and average net N₂O production/consumption rates (bar charts) in the MABR biofilm (A: DO profile; C: N₂O profile) and CBR biofilm (B: DO profile; C: N₂O profile). Note that net N₂O production (positive value) and consumption (negative value) rates (g-N/cm³/h) are based on biofilm volume. The measurement was carried out during operation days 90–95. The point at 0 μm represents the biofilm base.

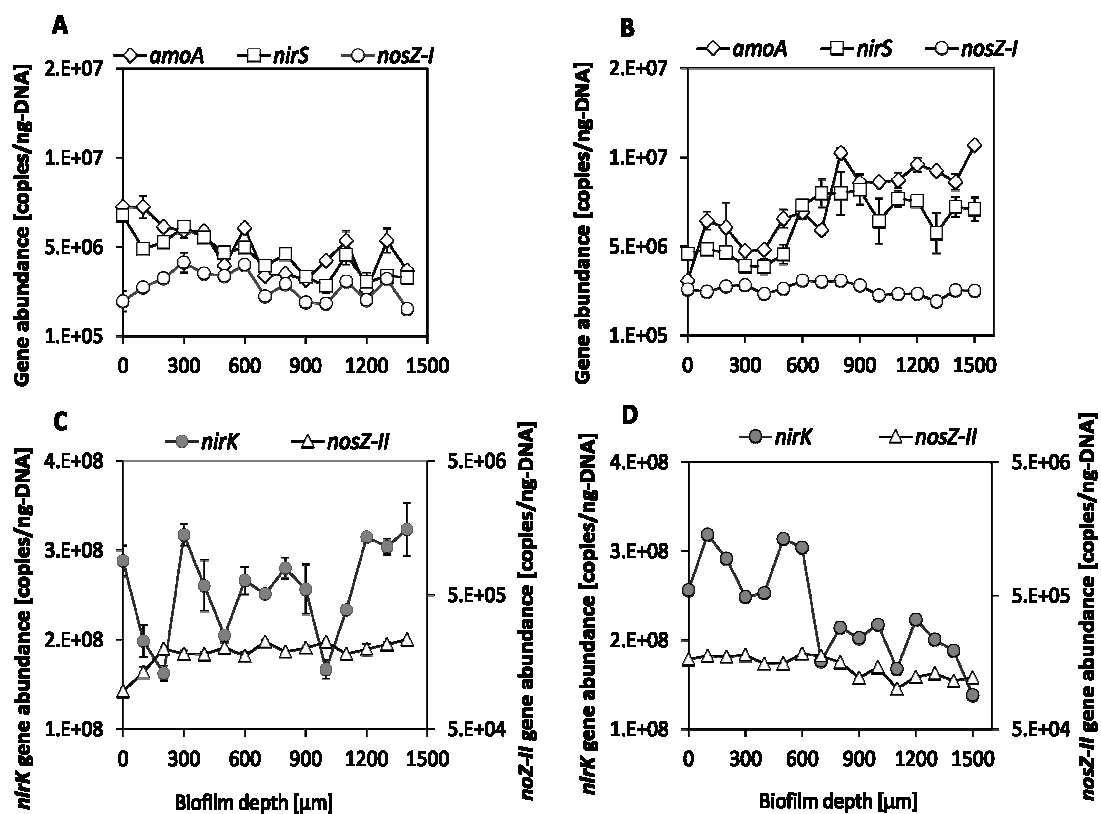


Figure 3. Depth profiles of functional genes for AOB (*amoA*) and denitrification (*nirS*, *nirK*, clade I *nosZ*, and clade II *nosZ*) in the biofilms of the MABR (A and C) and CBR (B and D).

The point at 0 μm represents the biofilm base.

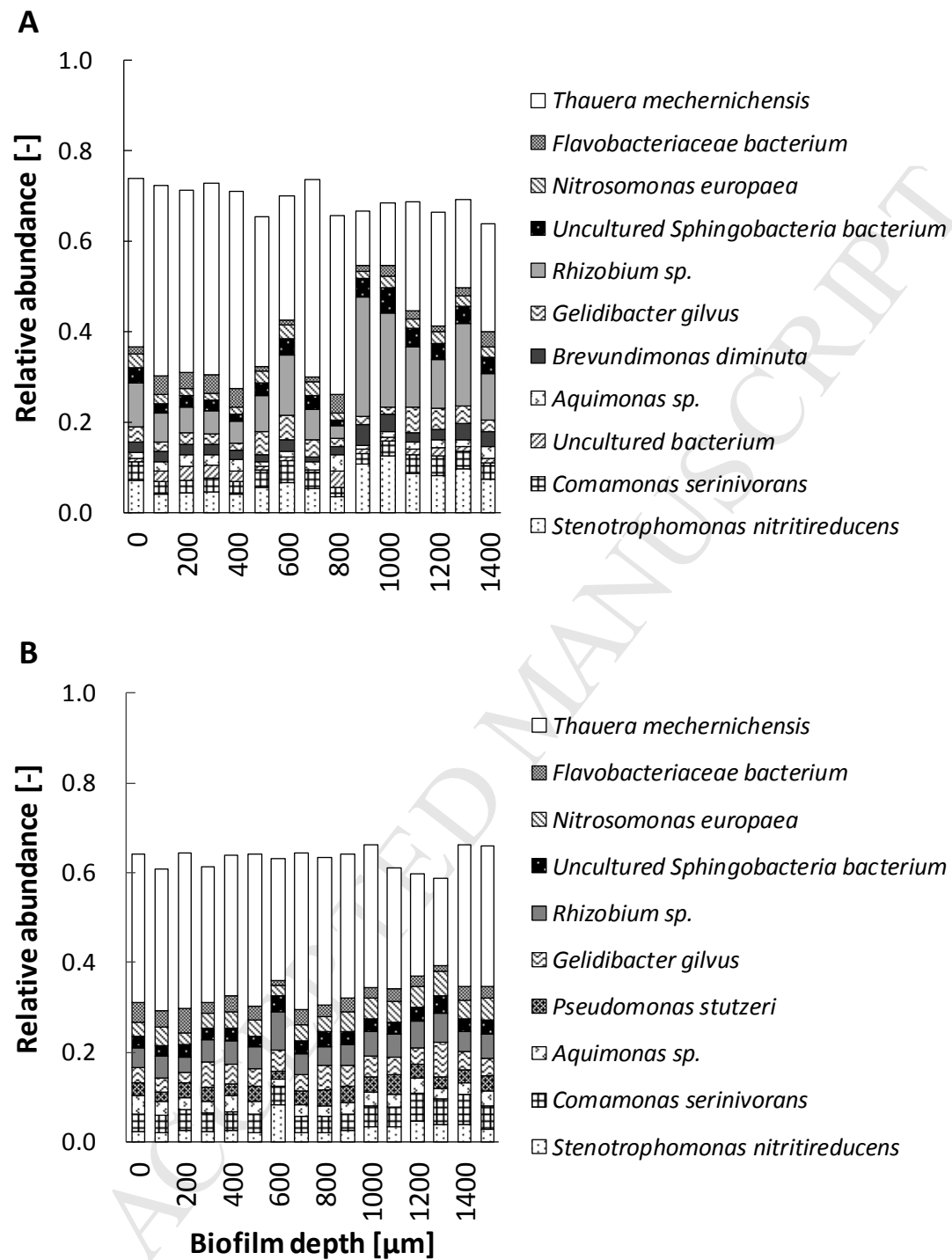


Figure 4. Depth-profile of relative bacterial abundance at the OTU level in the biofilms of the MABR (A) and CBR (B). All OTUs detected at least in one biofilm depth at $\geq 3\%$ relative abundance are shown. The point at 0 μm represents the biofilm base.

Highlights

- Depth profiles of N_2O and microbial community were compared between a MABR and CBR.
- Dissolved N_2O level was two orders of magnitude lower in the MABR than the CBR.
- Zones for N_2O production and consumption were close together in the MABR biofilm.
- Key N_2O -reducing bacteria, which may contribute to N_2O mitigation, were identified.